GMR Genetics and Molecular Research
Online Journal
ISSN:1676-5680

^{1}H-MRS before and after resuscitation following selective cerebral ultra-profound hypothermic blood flow occlusion in monkeys

X.-Q. Niu[1]*, X.-X. Zhao[2]*, B.-C. Li[3]*, Y.-J. Gao[4], W. Xu[4], Y.-D. Fan[4], G.-P. Fu[4], K. Wang[4] and J. Pu[4]

[1]Department of Respiratory Medicine,
Second Hospital of Kunming Medical University, Kunming, China
[2]Department of Radiology,
Second Hospital of Kunming Medical University, Kunming, China
[3]Department of Neurosurgery, Puer Central Hospital, Puer, China
[4]Department of Neurosurgery,
Second Hospital of Kunming Medical University, Kunming, China

*These authors contributed equally to this study.
Corresponding author: J. Pu
E-mail: punjun2@163.com

Genet. Mol. Res. 14 (4): 12595-12605 (2015)
Received May 27, 2015
Accepted August 24, 2015
Published October 19, 2015
DOI http://dx.doi.org/10.4238/2015.October.19.3

ABSTRACT. We investigated the effect of selective cerebral ultra-profound hypothermic blood flow occlusion on brain tissue and cell metabolism to ascertain the efficacy and safety of selective deep hypothermic technologies using proton magnetic resonance spectroscopy (^{1}H-MRS). The bilateral carotid artery was blocked at room temperature for 10 min. Other neck vessels were then blocked through cold perfusion of the internal carotid artery and reflux of the ipsilateral jugular vein. Thus, selective cerebral extracorporeal circulation was established. Brain temperature was reduced to 15.1° ± 0.9°C. After 60 min, cerebral blood flow recovered naturally. Routine magnetic resonance imaging

 ©FUNPEC-RP www.funpecrp.com.br

(MRI), diffusion-weighted imaging (DWI), and ^{1}H-MRS examination of the bilateral frontal cortex and basal ganglia were performed prior to surgery and 4, 24, 72 h, 21 days after recovery. The formants and areas under the curve (AUC) of *N*-acetyl aspartate (NAA), choline (Cho), creatine/phosphocreatine (Cr/Cr2) were analyzed using ^{1}H-MRS. The pre- and postoperative AUC of NAA and Cho at different time points were compared. Conventional MRI and DWI showed no abnormal signal changes in the brain parenchyma or right basal ganglia before and after surgery ($P > 0.05$). There was no significant difference in the ratio between NAA/(Cr+Cr2) and Cho/(Cr+Cr2) before and after surgery in the bilateral basal ganglia and frontoparietal regions of the cortex ($P > 0.05$). Quantitative ^{1}H-MRS showed that selective deep cerebral hypothermia significantly improved the brain's tolerance to ischemia and hypoxia. Our results could provide a better understanding of the efficacy and safety of selective deep hypothermia and blood flow occlusion.

Key words: Macaque monkey; Magnetic resonance spectroscopy; Hypothermia; Biochemical metabolism

INTRODUCTION

Previous studies have shown that selective deep cerebral hypothermia can improve the tolerance of the brain to ischemia and hypoxia with no obvious damage to major organs of the body (Jiang et al., 2003); however, the biochemical metabolism of brain tissue before and after selective deep cerebral hypothermia and blood flow occlusion is currently unknown. Proton magnetic resonance spectroscopy (^{1}H-MRS) enables quantitative analysis of biochemical changes in brain tissue and can detect cerebral ischemia or infarction earlier than conventional magnetic resonance imaging (MRI).

Currently, magnetic resonance spectroscopy (MRS) is the only non-invasive *in vivo* method for imaging tissue metabolism. It is based on the concentration, natural abundance, and MR sensitivity of nuclei in tissue. It can detect specific nuclei in tissues without causing any damage. Changes can then be assessed on a biochemical and genetic level; therefore, it is referred to as a virtual biopsy (Ende et al., 1997; Ju et al., 2004). Due to its natural abundance, inductivity, and high MRS sensitivity, ^{1}H is often used to detect a variety of trace metabolites, including *N*-acetyl aspartate (NAA), choline (Cho), creatine/phosphocreatine (Cr/Cr2), GLX complexes (glutamine, glutamate, and γ-amino butyric acid), lactate, and lipids. In the normal mammalian brain, NAA is exclusively found in neurons and their projections (dendrites and axons) and is recognized as an internal standard reflecting neuronal function. Cho is associated with cell membrane synthesis and is the main component for acetylcholine synthesis (Kraus et al., 2002). Therefore, changes in expression of NAA and Cho may reflect the changes in neuronal density, activity, and cell membrane structure. In this study, the ratios of NAA/(Cr+Cr2) and Cho/(Cr+Cr2) before and after recovery from selective deep cerebral hypothermic blood flow occlusion were investigated in monkeys to achieve a greater understanding of cerebral biochemical metabolism before and after this procedure.

MATERIAL AND METHODS

Experimental animals

Four healthy adult Rhesus monkeys were purchased from the Experimental Center of CAS Kunming Animal institute, male (N = 2) or female (N = 2), weighing 7.4-11 kg (mean weight = 9.4 kg).

Establishment of the model

After the induction of anesthesia (ketamine hydrochloride 10 mg/kg, diazepam 1 mg/kg), superficial venous access was established and a multi-channel physiological monitor was connected. Endotracheal intubation was conducted to maintain spontaneous breathing (100% oxygen). Anesthesia was maintained with intravenous instillation of propofol (0.1-0.2 $mg \cdot kg^{-1} \cdot min^{-1}$). Physiological conditions were monitored with an indwelling catheter, rectal thermometer, and electroencephalogram electrodes. A cannula was intubated at the proximal end of the right groin artery to monitor mean arterial pressure, one cannula was intubated at the proximal end of the right groin vein for recycling circulating blood in hypothermic perfusion, and one was intubated at the proximal end of the left groin vein for reinfusing circulating blood after rewarming. A cannula was intubated at the distal end of the right internal carotid artery and jugular vein to connect the rewarming ultrafiltration device (blood pump, fiber dialyzer connected with suction, heat exchanger with variable-temperature water tank, and corresponding connecting conduit) to establish local circulation. A cannula was intubated at the proximal end of the right internal jugular vein to measure central venous pressure. A brain temperature-sensor needle, connected to a temperature monitor, was inserted into the right frontal lobe. Prior to cooling, the monkey was systemically heparinized. Following occlusion of the external bilateral jugular vein, left internal carotid artery, and internal jugular vein, 10 min of ischemia was performed at room temperature. Ringer's solution (2-4 mL) was infused into the right carotid artery through the cooling system, maintaining a perfusion rate of 10 $mL \cdot kg^{-1} \cdot min^{-1}$. The perfusate was refluxed from the head of the right internal jugular vein and the circulating blood was recovered from the left groin vein. After removing the water using an ultrafilter, blood was rewarmed to 38°C and reinfused into the left groin vein. When the brain temperature dropped to ≤16°C, the input rate was reduced or intermittent cold perfusion was conducted. After maintaining the brain temperature for 60 min, low perfusion was stopped and normal blood flow to the blood vessel was recovered to naturally rewarm the brain via ligation of the right carotid artery and vein. Water retention was filtered *in vivo* and the remaining blood in the rewarming ultrafiltration apparatus was slowly reinfused. Central venous pressure was maintained at no more than 10 cmH_2O and core body temperature was returned to normal as soon as possible. Protamine (1:1) was used to antagonize the anticoagulant effects of heparin. The surgical incisions were sutured. When the rectal temperature returned to 35°C and breathing was steady, intubation was removed and the monkey was allowed to recover naturally.

MRI examination

MR equipment and sequences

We used a Siemens sonata 1.5 T superconducting MR imaging system with a standard

head coil as the transmitter and receiver coil. Before the ^{1}H-MRS, all animals underwent conventional MRI, including T1 (T1WI) and T2 weighted imaging (T2WI), and fast fluid attenuated inversion recovery (FLAIR) scans, and diffusion-weighted imaging (DWI). A spin-echo sequence was used for T1WI, including the horizontal (Tra) and sagittal (Sag) axes. T2WI was performed using turbo spin echo sequences, including the Tra axis. DWI was conducted using the Tra axis with the diffusion-sensitive gradient b = 1000 s/mm^2. Average diffusion images and apparent diffusion coefficient (ADC) maps were automatically generated using the Via 2.0 software. Twelve and 11 layers were scanned axially and sagittally, respectively. The thickness and interlayer spacing was 4 and 0.08 mm, respectively. The matrix was 256-512 x 256-512. Routine MRI, DWI, and ^{1}H-MRS examination of the bilateral frontal cortex and basal ganglia were performed before surgery and 4, 24, 72 h, and 21 days after surgery.

Before ^{1}H-MRS examination, T2WI unenhanced images in Tra, Sag, and coronal (Cor) orientation were collected for voxel positioning. ^{1}H-MRS was performed using stimulated echo acquisition (STEAM), chemical shift selective saturation (CHESS) and single-voxel spectroscopy (SVS). A point resolved spectroscopy (PRESS) sequence was used for SVS acquisition of regions of interest (ROIs). Positioning technology used for image selected *in vivo* spectroscopy (ISIS), which used unenhanced MRI images (including three azimuth of Tra, Sag, and Cor) to locate the MRI, avoiding the cerebrospinal fluid of scalp tissue ventricles and cerebral sulci. TE: 135 ms, TR: 1500 ms, flip angle: 90°, number of excitations: 200, collection frequency: 128. The ROI size of the bilateral basal ganglia: 10 x 10 x 10 mm, ROI size of the bilateral frontoparietal cortex: 10 x 15 x 15 mm. The acquisition time for each ROI was 6 min 21 s. Baseline and phase correction were conducted after spectra were obtained.

Statistical analysis

SPSS 12.0 was used to analyze the data. Measurement data are reported as means ± SD. Comparisons at different time points before and after surgery were analyzed using ANOVA with α set at 0.05. $P < 0.05$ was considered to be statistically significant.

RESULTS

Performance of conventional MRI and DWI

Comparisons of T1WI, T2WI, FLAIR, and DWI before surgery and 4, 24, 72 h, 21 days after recovery showed no abnormal signal changes in the brain parenchyma or ischemic brain changes in DWI and ADC maps (Tables 1 and 2).

Table 1. ANOVA of the NAA/(Cr+Cr2) ratio in the bilateral basal ganglia and bilateral frontoparietal cortex before and after surgery.

Region	Preoperative	Postoperative 4 h	Postoperative 24 h	Postoperative 72 h	Postoperative 21 days	*F*-value	P value
Right basal ganglia	0.93 ± 0.22	0.69 ± 0.28	0.78 ± 0.22	0.84 ± 0.39	0.80 ± 0.30	0.356	0.835
Left basal ganglia	1.09 ± 0.27	0.71 ± 0.37	1.27 ± 0.65	0.80 ± 0.24	0.92 ± 0.40	1.405	0.291
Right frontoparietal cortex	1.28 ± 0.75	1.19 ± 0.54	1.48 ± 0.20	1.64 ± 0.50	0.91 ± 0.32	2.085	1.460
Left frontoparietal cortex	1.15 ± 0.68	1.53 ± 0.92	1.24 ± 0.34	2.11 ± 1.97	1.04 ± 0.38	0.606	0.666

Data are reported as means ± SD. There was no significant difference in the NAA/(Cr+Cr2) ratio in the bilateral basal ganglia and bilateral frontoparietal cortex before and after surgery.

Table 2. ANOVA of the Cho/(Cr+Cr2) ratio in the bilateral basal ganglia and bilateral frontoparietal cortex before and after surgery.

Region	Preoperative	Postoperative 4 h	Postoperative 24 h	Postoperative 72 h	Postoperative 21 days	*F*-value	P value
Right basal ganglia	0.50 ± 0.20	0.43 ± 0.09	0.38 ± 0.13	0.47 ± 0.18	0.40 ± 0.12	0.680	0.620
Left basal ganglia	0.45 ± 0.09	0.41 ± 0.12	0.40 ± 0.12	0.51 ± 0.32	0.30 ± 0.17	0.680	0.620
Right frontoparietal cortex	0.32 ± 0.16	0.30 ± 0.13	0.28 ± 0.17	0.35 ± 0.28	0.34 ± 0.22	0.065	0.991
Left frontoparietal cortex	0.18 ± 0.04	0.24 ± 0.08	0.79 ± 0.92	0.19 ± 0.08	1.04 ± 0.38	1.403	0.291

Data are reported as means ± SD. There was no significant difference in the Cho/(Cr+Cr2) ratio in the bilateral basal ganglia and bilateral frontoparietal cortex before and after surgery.

Figure 1 shows the preoperative MRI, Figure 2 shows the MRI 24 h post-surgery. Figure 3 shows the preoperative DWI. Figure 4 shows the DWI 4 h post-surgery. Figure 5 shows the preoperative spectrum of the right frontoparietal cortex. Figure 6 shows the positioning map. Figure 7 shows the spectrum of right frontoparietal near cortex 4 h post-surgery. Figure 8 shows the positioning map. Figure 9 shows the spectrum of right frontoparietal cortex 24 h post-surgery. Figure 10 shows the location map.

The metabolites detected by [1]H-MRS and the position formant

Seven peaks appeared in the [1]H-MRS analyses (Figure 5): NAA, Cr2, Cr, Cho, GLXm1, GLXm2, and GLXm3 (the three GLX peaks will be discussed in a different paper). The highest peak was that of NAA and this was located at 1.95-2.08 ppm (Figure 7). The second highest peak was Cr and it was located at 3.16-3.25 ppm (Figure 9). The Cho resonance peak was located at 3.01-3.10 ppm. The Cr2 resonance peak located at 3.86-3.98 ppm. The absolute quantification of [1]H-MRS was difficult. The content of Cr and Cr2 in the brain are more stable; therefore, Cr+Cr2 served as a reference to distinguish any changes in NAA and Cho. There was no difference in NAA and Cho in the ROIs. Every ROI of each monkey was assessed before surgery, and 4, 24, 72 h, and 21 days after surgery (20 times in four monkeys).

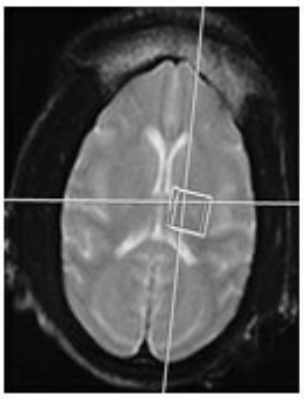

Figure 1. Preoperative magnetic resonance imaging.

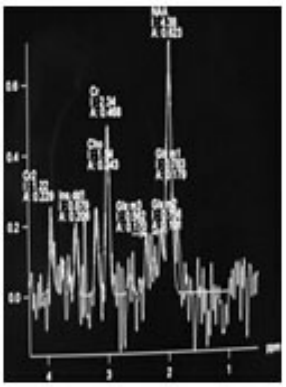

Figure 2. Magnetic resonance imaging 24 h after surgery.

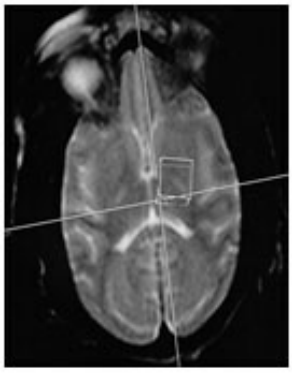

Figure 3. Preoperative diffusion-weighted imaging.

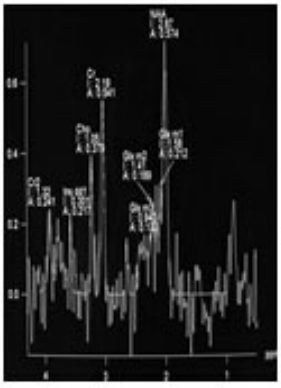

Figure 4. Diffusion-weighted imaging 4 h after surgery.

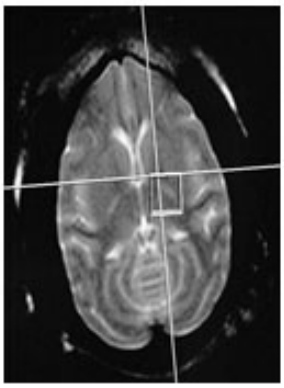

Figure 5. Preoperative spectrum of the right frontoparietal cortex.

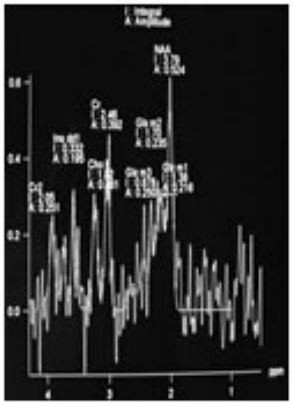

Figure 6. Positioning map.

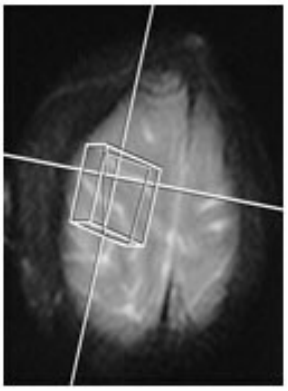

Figure 7. Spectrum of the right frontoparietal cortex 4 h after surgery.

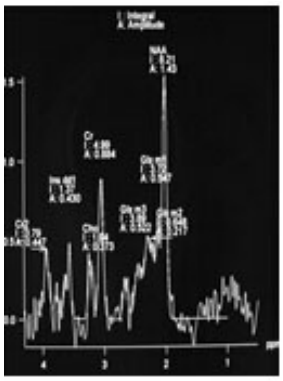

Figure 8. Positioning map.

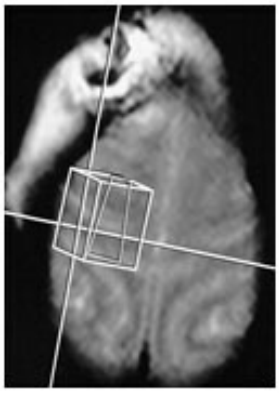

Figure 9. Spectrum of the right frontoparietal cortex 24 h after surgery.

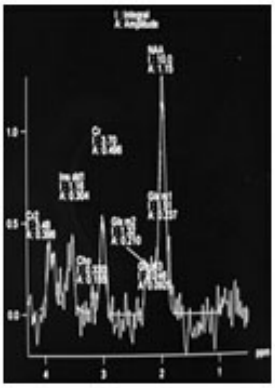

Figure 10. Location map.

DISCUSSION

In the present study, we investigated the effect of selective cerebral ultra-profound hypothermic blood flow occlusion on brain tissue and cell metabolism to ascertain the efficacy and safety of selective deep hypothermic technologies using [1]H-MRS.We found that there was no significant difference in the ratio between NAA/(Cr+Cr2) and Cho/(Cr+Cr2) before and after surgery in the bilateral basal ganglia and frontoparietal regions of the cortex ($P > 0.05$). Quantitative [1]H-MRS showed that selective deep cerebral hypothermia significantly improved the brain's tolerance to ischemia and hypoxia. Our results could provide a better understanding of the efficacy and safety of selective deep hypothermia and blood flow occlusion.

Pathological basis of the monkey selective deep cerebral hypothermia occlusion recovery model

Previous studies have shown that there is no significant change in enzyme function in the heart, kidney, liver, and other organs in this animal model. No abnormal morphology is detected by hematoxylin-eosin staining. Electron microscopy of cellular ultrastructures has shown normal neuronal morphology of brain cells, including the absence of abnormal organelles. In addition, there are no changes in apoptotic or necrotic tissue dissolution (Xu et al., 2003).

Changes in NAA and Cho before and after selective cerebral hypothermia blood flow occlusion in the monkey brain

The brain has the highest metabolic demands in the body; it occupies approximately 2% of body weight and cerebral blood flow accounts for approximately 15% percent of the heart excretion in a resting state. Oxygen consumption accounts for approximately 20% of total body oxygen consumption. Subsequently, it is very sensitive to ischemia and hypoxia. Research has shown that a 1°C drop in body temperature decreases metabolic levels by 5%. When the body temperature drops to 15°C, the metabolic rate is 10% that of the normal metabolic rate. When the human brain temperature drops to 23°C, the brain metabolic rate reduces to 25% of the normal metabolic rate. Therefore, hypothermia can be protective in hypoxic conditions (Cancio et al., 1994). Animal experiments and clinical studies have shown that systemic deep hypothermia can lead to irreversible pathological damage of the heart, lungs, and other organs, and eventually cause death (Lu et al., 2000). However, selective cryogenic technology provides an ultra-deep hypothermic state for the brain and does not affect vital organs, such as the heart and lungs.

MRS has been used clinically since 1988. Based on MRI, this non-invasive technology, which measures biochemical changes in the central nervous system, attracts more and more attention. [1]H has a high natural abundance, inductivity, and MRS detection sensitivity; therefore, it has been widely used in analyses of ischemic cerebral infarction, epilepsy, brain tumors, Parkinson's disease, and Alzheimer's disease (Frahm et al., 1989).

NAA is formed by L-aspartic acid and acetyl coenzyme A in mitochondria and transported to the cytoplasm of neurons, where it accumulates. NAA is recognized as a marker of neuronal density and activity, which has been confirmed by histology, cytology, and specific antibody tests in clinical studies (Ciccarelli et al., 2001). Cho, the main component of acetylcholine, correlates with the formation of the cell membrane. Changes in NAA are more

sensitive and detected earlier in cerebral ischemic infarction when compared with conventional MRI. Animal studies have shown that the level of NAA is significantly reduced (approximately 25% of baseline) after 1.3 h after infarction (Demougeot et al., 2002). Wardlaw et al. (1998) have found that patients with infarctions do not exhibit obvious changes upon MRI examination within 4 h of presentation, whereas the changes using MRS are very evident. Graham et al. (1995) have analyzed 32 cases of patients with stroke and found that NAA is reduced in early ischemia. In line with this, Federico et al. (1999) found that the NAA content declines after 2 h of brain ischemia and its decline is closely correlated to the area of infarction. Lauriero et al. (1996) believed that the decline in NAA is closely related to blood flow in acute and chronic cerebral ischemia and a greater decline in NAA indicates a worse prognosis. These studies suggest that NAA content is an important outcome indicator for stroke patients. Further evidence comes from a study showing that the decline in NAA is positively correlated with the severity of symptoms (Federico et al., 1996). In addition, NAA content is significantly decreased in patients with subcortical cerebral infarction (Lai et al., 1995). In early ischemia, NAA increases within the infarction, while the T2WI is generally normal (Barker et al., 1994). Gideon et al. (1992) hypothesized that there was no significant difference in Cho content in infarct areas and normal brain tissue. Nonetheless, many researchers believe that in the acute phase of ischemic infarction Cho content decreases while that of NAA does not change. This may be because neurons are more sensitive to ischemia when compared with glial cells (Asono, 1998). Duijn et al. (1992) found an approximate 54% decrease in Cho content in early cerebral ischemia and infarction; however, it has been suggested that Cho content increases in the infarct. This may be associated with the degradation of cell membranes or demyelination of axons (Scremin and Jenden, 1989).

In summary, NAA and Cho are sensitive and reliable indicators that reflect the activity of neuronal densities and changes in the structure of cell membranes in cerebral infarction. This study showed that there was no significant difference in NAA and Cho content in the bilateral frontoparietal cortex and basal ganglia in the monkey brain before and after ultra-deep hypothermia at different time points. Conventional MRI and DWI did not show any ischemic infarction. This further validated the safety and efficacy of selective hypothermia on the monkey brain using blood flow technology to assess radiological and biochemical metabolic changes.

REFERENCES

Asono T (1998). Clinical application of 1H nuclear magnetic resonance spectroscopy into patients with cerebral ischemia. *Hokkaido Iguku Zasshi* 73: 581-597.

Barker PB, Gillard JH, Vanziji PC, Soher BJ, et al. (1994). Acute stroke: evaluation with serial proton MR spectroscopic imaging. *Radiology* 192: 723-732.

Cancio LC, William WG and Zimba F (1994). Hypothermia in acute blunt head injury. *Resuscitation* 28: 9-16.

Ciccarelli O, Werring DJ, Wheeler-Kingshott CA, Barker GJ, et al. (2001). Investigation of MS normal-appearing brain using diffusion tensor MRI with clinical correlations. *Neurology* 56: 926-933.

Demougeot C, Walker P, Beley A, Marie C, et al. (2002). Spectroscopic data following stoke reveal tissue abnormality beyond the region of T2-weighed hyperintensity. *J. Neurol. Sci.* 199: 73-78.

Duijn JH, Maston GB, Maudsley AA, Hugg JW, et al. (1992). Human brain infarction: proton MR spectroscopy. *Radiology* 183: 711-718.

Ende GR, Laxer KD, Knowlton RC, Matson GB, et al. (1997). Temporal lobe epilepsy: bilateral hippocampal metabolite changes revealed at proton MR spectroscopic imaging. *Radiology* 202: 809-817.

Federico F, Simone IL, Conte C, Lucivero V, et al. (1996). Prognostic significance of metabolic changes detected by

proton magnetic resonance spectroscopy in ischemic stroke. *J. Neurol.* 243: 241-247.
Federico F, Simone IL, Lucivero V, Giannini P, et al. (1999). Prognostic value of proton magnetic resonance spectroscopy in ischemic stroke. *Arch. Neurol*. 55: 489-494.
Frahm J, Bruhn H, Gyngell ML, Merboldt KD, et al. (1989). Localized high-resolution proton NMR spectroscopy using stimulated echoes: initial applications to human brain *in vivo*. *Magn. Reson. Med.* 9: 79-93.
Gideon P, Henriksen O, Sperling B, Christiansen P, et al. (1992). Early time course of *N*-acetylasparate, creatine and phosphocreatine, and compounds containing choline in the brain after acute stroke a proton magnetic resonance spectroscopy study. *Stroke* 23: 1566-1572.
Graham GD, Kalvach P, Blamire AM, Brass LM, et al. (1995). Clinical correlates of proton magnetic resonance spectroscopy findings after acute cerebral infarction. *Stroke* 26: 225-229.
Jiang JX, Xu W, Yang PF, Fang X, et al. (2003). Selective deep cryogenic technology study of monkey carotid artery block time limit. *Chin. J. Neurosurg*. 19: 304-306.
Ju SH, Chen F, Teng GJ, Liu Z, et al. (2004). MR monomer element spectrum and chemical shift imaging research in temporal lobe epilepsy. *Chin. J. Radiol.* 38: 1180-1185.
Kraus J, Kuehue BS, Tofighi J, Frielinghaus P, et al. (2002). Serum cytokine levels do not correlate with disease activity and severity assessed by brain MRI in multiple sclerosis. *Acta Neurol. Scand.* 105: 300-308.
Lai ML, Hsu YI, Mu S and Yu CY (1995). Magnetic resonance spectroscopic findings in patients with subcortical ischemic stroke. *Zhonghua Yi XueZaZhi* 56: 31-35.
Lauriero F, Federico F, Rubini G, Conti C, et al. (1996). 99mTc-HMPAO SPECT and [1]H-MRS (proton magnetic spectroscopy) in patients with ischemic cerebral infarction. *Nucl. Med. Commun.* 17: 140-146.
Lu HL, Jiang JX, Zhu C, Meng M, et al. (2000). Dog brain selective deep low temperature impact on the important organs physiological function of body. *J. Second Mil. Med. Univ.* 21: 272-274.
Scremin OU and Jenden DJ (1989). Effects of middle cerebral artery occlusion on cerebral cortex choline and acetylcholine in rats. *Stroke* 20: 1524-1530.
Wardlaw JM, Marshall I, Wild J, Dennis MS, et al. (1998). Studies of acute ischemic stroke with proton relation between time from onset neurological deficit metabolite abnormalities in the infarct blood flow and clinical outcome. *Stroke* 29: 1618-1624.
Xu W, Gao YJ, Sun L, Niu L, et al. (2003). Monkey selective deep low temperature for the whole body main organs function image. *J. Kunming Med. Coll.* 2: 6-9.